

Measurements of Short-Lived Isomers from Photofission as a Method of Active Interrogation for Special Nuclear Materials

S.W. Finch^{1,2,*}, M. Bhike,^{1,2} C.R. Howell^{1,2}, Krishichayan^{1,2}, W. Tornow,^{1,2} A.P. Tonchev,^{3,1} and J.B. Wilhelmy^{1,4}

¹*Department of Physics, Duke University, Durham, North Carolina 27708, USA*

²*Triangle Universities Nuclear Laboratory, Durham, North Carolina 27708, USA*

³*Lawrence Livermore National Laboratory, Livermore, California 94550, USA*

⁴*Los Alamos National Laboratory, Los Alamos, New Mexico 87545, USA*



(Received 6 August 2020; revised 26 January 2021; accepted 17 February 2021; published 12 March 2021)

Isomeric fission products, such as ^{134m}Te ($T_{1/2} = 164$ ns) and ^{136m}Xe ($T_{1/2} = 2.95$ μs), are proposed as a signature of special nuclear materials in active interrogation applications. To test this conjecture, monoenergetic 9, 11, and 13 MeV photons from the HI/S facility are used to induce fission of ^{235}U , ^{238}U , and ^{239}Pu targets. The de-excitation γ rays of the isomers are measured using time-gated spectroscopy with high-purity germanium detectors. The ^{134m}Te and ^{136m}Xe isomers are detected and identified by the energy and decay half-life of their characteristic γ -ray transitions. The ratio of yields for these two signature γ rays, corresponding to $^{134m}\text{Te}/(^{136m}\text{Xe} + ^{136}\text{I})$, is found to be strongly correlated with the identity of the fissioning nuclei. These results show that fission-product isomers may be used in active interrogation to detect and identify special nuclear materials, even providing information on the isotopic enrichment. The feasibility of an active interrogation scenario using a bremsstrahlung beam is discussed.

DOI: 10.1103/PhysRevApplied.15.034037

I. INTRODUCTION

Nuclear fission is a process in which the nucleus becomes strongly deformed and then ruptures into two fragments, releasing a large amount of energy. The released energy in fission is converted mostly into kinetic energy of the fragments [1]. The majority of the remaining excitation energy will be distributed among neutrons and γ rays. The primary angular momentum of the nascent fragments is an important observable for characterizing the fission process, as it dictates the number of emitted neutrons and photons. During the final stage of the fission process, the fission products are emitted with an average of 7 ± 2 units of total angular momentum (combined orbital angular momentum and spin) [2,3]. Neutron emission is expected to decrease the spin of the fragments by on the order of one unit of angular momentum, while γ -ray emission dissipates the remaining spin of the fragments [4]. The number and multipolarity of the γ rays emitted by the fragments depends on the resultant spin of the fragment following neutron emission. The large kinetic energy and angular momentum of the emitted fragments suggest that the fission fragments are produced in excited nuclear states, including isomeric states. The production of fragments in isomeric states opens up the possibility of

using activation techniques to measure the fission yields. Currently, the only fission-product yield (FPY) data of very short-lived isomeric decays exists for the spontaneous fission of ^{252}Cf [5,6].

In this paper, we investigate the production of ^{134}Te and ^{136}Xe via photofission of ^{235}U , ^{238}U , and ^{239}Pu . These products are both even-even $N = 82$ closed-shell nuclei with a $J^\pi = 0^+$ ground state. Both nuclei have a 6^+ excited state that is sufficiently close in energy to the lowest 4^+ state, which, combined with nuclear structure factors, hinders the decay. This configuration results in an isomeric 6^+ state of $T_{1/2} = 164$ ns for ^{134m}Te [7] and 2.95 μs for ^{136m}Xe [8]. The isomeric state decays through the $6^+ \rightarrow 4^+ \rightarrow 2^+ \rightarrow 0^+$ sequential γ -ray cascade, as shown in Fig. 1. The $2^+ \rightarrow 0^+$ decay produces a high-energy γ ray that can penetrate shielding materials and form the characteristic signal of the isomeric decay. The emission of time-delayed γ rays from ^{134m}Te post fission is predicted theoretically by the Monte Carlo fission code CGMF [9].

These isomeric transitions may be used for active interrogation of special nuclear materials. Current techniques utilizing passive detection have difficulty discriminating between different isotopic concentrations; specifically, between uranium isotopes. Techniques for active interrogation involve an incident probe, usually a photon or neutron beam, and detection of particles emitted from induced nuclear reactions that can be used to infer the target nucleus

* sfinch@tunl.duke.edu

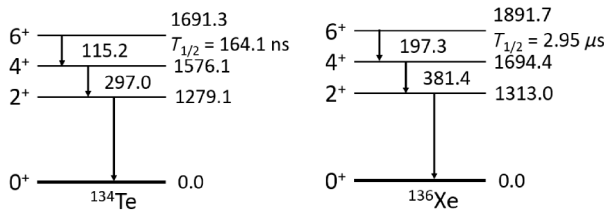


FIG. 1. The level diagrams for the decay of the isomeric 6^+ states of ^{134}Te and ^{136}Xe .

[10,11]. Of these two probes, photons are preferred over neutrons because they induce lower radioactivity in most materials. The characteristic signal may either be prompt or delayed radiation. Prompt γ -ray signatures include nuclear-resonance fluorescence [12,13]. Methods based on prompt γ -ray detection typically have the challenge of dealing with a low signal-to-background ratio, as beam-induced backgrounds are temporally coincident with the signal of interest. In the case of nuclear-resonance fluorescence, the signal γ rays are temporally coincident with any beam photons that Compton scatter or pair produce on atomic electrons in the materials. In addition, the nuclear states in actinide nuclei excited via nuclear-resonance fluorescence have a relatively small decay width on the order of 10–50 meV [14,15]. These decay widths are 3–5 orders of magnitude smaller than some strong resonance states in lead isotopes, for example. These problems can be alleviated by observing delayed radiation, which occurs after the incident beam pulse. Typical proposals for identifying fissile materials involve detection of β -delayed γ rays [16–18] and neutrons [19,20]. Beta-delayed processes occur with a mean lifetime on the order of seconds following fission. Interrogation of materials based on methods that use production of the isomers studied in this work offer an alternative to detecting β -delayed particles from fission and the possibility of developing technologies that use dual-signature identification to reduce the rate of false positives. Detection of a substantial fraction of the β -delayed neutrons and γ rays and measurement of their characteristic decay curve require counting periods of seconds following the incident beam pulse on the material, while efficient detection of the isomers discussed in this work can be achieved with a counting period 5 orders of magnitude shorter, thus greatly enhancing the duty factor of the probe. This feature requires the use of time-gated spectroscopy in applications of beam-based material interrogation. The short counting time scale allows for the use of high-duty-cycle beams, resulting in a larger flux over shorter measurement periods than applications with data windows on the order of seconds. Also importantly, the time scale for applying isomeric detection is compatible with that used in active interrogation methods based on prompt neutron measurements [21–23]. Prompt neutron measurements are highly sensitive to the detection

of actinide nuclei but are prone to a higher false-positive rate than using delayed neutron or γ -ray detection and have difficulty providing information on the specific isotope undergoing fission. This problem might be improved by methods that use prompt neutron detection in the primary assay and isomeric identification as the secondary signature in cases of a positive reading by the primary method.

For the spontaneous fission of ^{252}Cf , the measured yields of the ^{134m}Te and ^{136m}Xe isomers are 1.26% per fission and 0.57% per fission, respectively [5]. These yields are comparable to the yield of delayed neutrons: 1.6% per fission for ^{235}U and 0.63% per fission for ^{239}Pu . ENDF/B-VIII.0 [24] provides evaluations of the independent FPY of neutron-induced fission. The independent yield of the two fission products ^{134}Te and ^{136}Xe in their ground state from neutron-induced fission of ^{232}Th , $^{233,235,238}\text{U}$, ^{239}Pu and spontaneous fission (sf) of ^{252}Cf is shown in Fig. 2(a). The ratio of the yields $^{134}\text{Te}/^{136}\text{Xe}$ is also shown in Fig. 2(b). This ratio enables two levels of discernment: (1) the ratio is significantly larger for the nonthermally fissile ^{232}Th and ^{238}U than for the more fissile nuclei ^{233}U , ^{235}U , and ^{239}Pu ; and (2) this ratio shows substantial specificity to the fission species, thus providing a possibility of characterization of the fissile isotopic composition of the interrogated material. Given that the isomeric 6^+ state is close in spin to the 7 ± 2 units of angular momentum released by fission, the isomeric states are likely highly populated and the discernment properties of the ratio could extend to the isomeric states as well. Note that these FPY predictions are for neutron-induced fission at $E_n = 0.5 \text{ MeV}$ (or spontaneous fission in the case of ^{252}Cf), and are expected to be representative of, but not identical to, the photofission-product yields being determined in the present work, which represent a different compound nucleus at a different excitation energy.

The ^{136m}Xe and ^{134m}Te isomers can be unambiguously identified by their unique decay time and energy signature. The production of these isomers is unique to the fission process, and the associated 1.3 MeV de-excitation γ rays have relatively high energies compared to most spectroscopy lines. Finally, the yield of these two isomers will provide information on the identity of the fissioning material.

II. EXPERIMENTAL METHOD

The experiment is conducted at the High Intensity γ -Ray Source (HI γ S) [25]. HI γ S produces monoenergetic photons by Compton backscattering of free-electron laser light. The photon beam is circularly polarized and collimated using a 1.905-cm-diameter Pb collimator. In the present work, beam energies are 9, 11, and 13 MeV, with a beam energy spread of approximately 200 keV full width at half maximum (FWHM). The photon beam has a pulsed

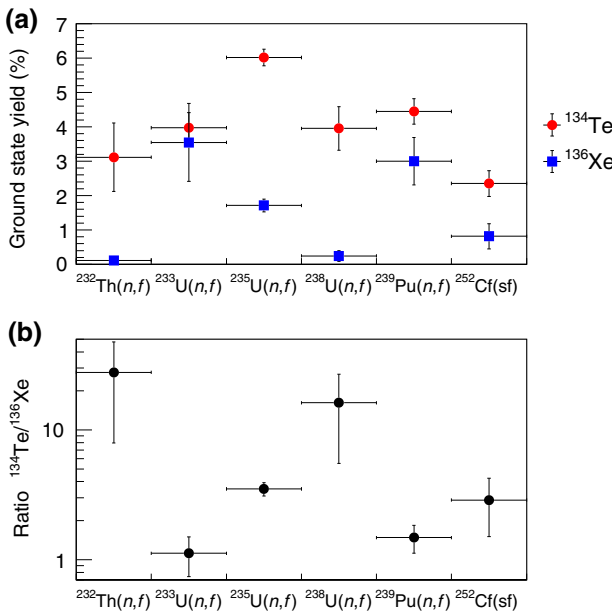


FIG. 2. ENDF/B-VIII.0 evaluations for the independent FPYs of ^{134}Te and ^{136}Xe in their ground state (a) and the ratio of the yields (b) for different fissioning actinides. All data are for neutron-induced fission at $E_n = 0.5$ MeV, except for ^{252}Cf , which is from spontaneous fission.

time structure with a 179-ns period between pulses and a pulse width of 310 ps FWHM. The incident photon flux on target is approximately $(1\text{--}4) \times 10^7 \gamma/\text{s}$, depending on the beam energy.

The targets are metal foils of 1-in. diameter and a mass of 2.1 g of natural abundance ^{238}U , 1.5 g ^{235}U enriched to 93.7%, and 0.47 g ^{239}Pu enriched to 98.4%. The de-excitation γ rays are measured by three 60% relative-efficiency coaxial high-purity germanium (HPGe) detectors. The three detectors are positioned at the backward angles of $\theta = 135^\circ$, $\phi = 0^\circ, 90^\circ, 270^\circ$ relative to the beam axis, in order to minimize the background from Compton scattering. To attenuate low-energy background γ rays, including 511 keV, 0.3-cm-thick copper followed by 0.6-cm-thick lead sheets are placed in front of the detector faces, between the detector and the actinide target. In addition, to shield the HPGe detectors from fission neutrons, a 2.5-cm-thick disk of high-density polyethylene is placed on each detector face on top of the lead disk. The actinide targets are positioned 15 cm from the front face of the HPGe detector. The shielding and distance configurations mimic configurations that might be present in active interrogation: the detectors are displaced by up to 3 m from the target and some intermediate shielding is present between the target and detectors [10]. In the present shielding situation, the signal γ rays (1.3 MeV) are attenuated by a factor of 1.9. Background γ rays, of primary energy 511 keV, created by the photon beam, are attenuated by a factor of 4.3 [26]. In this regard, the presence

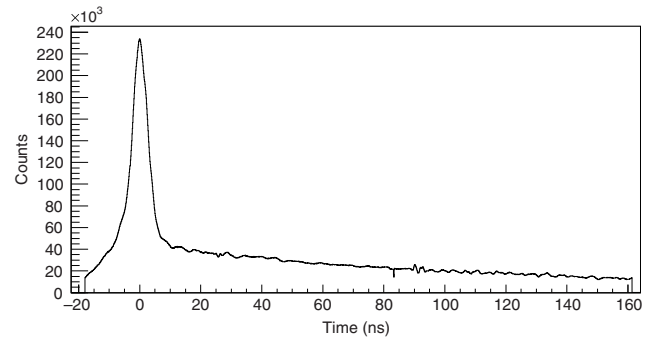


FIG. 3. The counts in a HPGe detector as a function of time relative to the beam pulse. The burst of γ rays from the beam pulse and prompt radiation is seen at $t = 0$, while the steady decay of delayed radiation is seen for $t > 10$ ns.

of shielding actually improves the gross detector count rate signal-to-background ratio by a factor of 2.2 for these isomeric transition γ rays. The full peak efficiency of all three HPGe detectors, summed together, is 0.093(3)% for 1279.1- and 1313.0-keV γ rays. This efficiency is low due to the small solid angle subtended by the HPGe detectors.

The signals from the HPGe detectors are collected and processed by a CAEN 12-bit analog-to-digital converter (ADC) and time-to-digital converter (TDC). In addition, the time of the beam pick-off signal is recorded to calculate the time of each detected γ ray relative to the HI γ S beam pulse. The data acquisition system records the energy and time, relative to the beam pulse, of each detected γ ray in a binary list file. The spectrum of counts relative to the beam pulse for a HPGe detector is shown in Fig. 3. The high prompt signal associated with the beam pulse is clearly seen. The detector count rate is much lower in the region between beam pulses, resulting in a higher signal-to-background ratio.

III. ANALYSIS

As the data are accumulated using list-mode electronics, different analysis procedures can be used. To aid in identifying the isomers, two γ -ray energy spectra are projected using two separate time windows: 16–82 ns and 128–162 ns after the beam pulse. The energy spectra accumulated with these time windows are shown in Fig. 4. As expected, the 1279.1-keV γ ray decays between beam pulses. We measure an average half-life of 143 ± 22 ns, consistent with the published value of 164 ± 1 ns [7]. The accuracy of the measured half-life is limited by systematic uncertainties due to the HI γ S beam time structure being comparable to the half-life. An additional ($T_{1/2} \approx 100$ ns) isomeric state is observed at 1326.7 ± 0.5 keV in all three actinide targets. This isomer, likely produced from fission, does not appear in the current National Nuclear Data Center database and merits additional study.

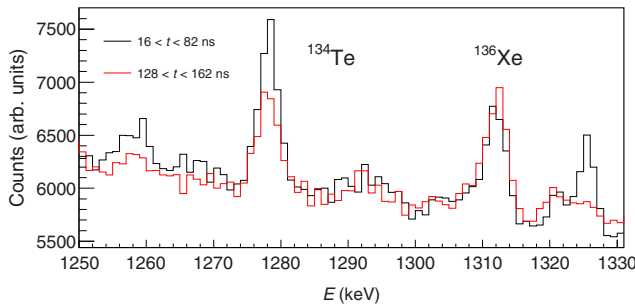


FIG. 4. Histograms of the measured energy spectra of the two γ rays emitted from the two isomeric transitions at different points in time. The decay of the ^{134m}Te isomer is observed. These spectra are taken following the irradiation of ^{238}U with $E_\gamma = 11$ MeV photons.

The 1313.0-keV γ ray from the longer-lived ^{136m}Xe shows no signs of decay during the time between beam pulses. This is expected, since the half-life of ^{136m}Xe is substantially larger than the beam pulsing period. In the case of ^{136m}Xe , the signal γ ray at 1313.0 keV is also produced from the β decay of ^{136}I and ^{136m}I with intensities of 66% and 100%, respectively [8]. Both ^{136}I and ^{136m}Xe are produced from fission in comparable amounts. As such, it is not possible for the present experiment to determine which fission product produces the 1313.0-keV γ ray. The present results report the yield of ^{136m}Xe plus the cumulative FPY of ^{136}I , i.e., the combined yields of $\text{FPY}(\text{Xe}) + \text{FPY}(\text{I})$, where ^{136}I then populates the 2^+ state of ^{136}Xe . The ^{136}I nucleus has a much longer half-life of 83.4 s, and 46.9 s for the isomeric state ^{136m}I . With a beam pulsing period greater than 3 μs , it would be possible to disentangle the contribution from ^{136m}Xe and ^{136}I . ^{134m}Te does not suffer any significant contamination from its parent nucleus, ^{134}Sb , which has an approximately 20 times lower FPY. Additionally, the γ -ray intensity for the 1279.1-keV γ ray from β decay of ^{134}Sb is only 1.1% [7]. The absence of ^{134}Sb is verified by our data, where the measured half-life is consistent with the expected value. If ^{134}Sb significantly contributed to the data, the measured half-life would be noticeably biased toward larger values. Lower-frequency beam pulsing would allow for improved measurements of $T_{1/2}$ for both isomers. Combined measurement of the energy and half-life of the γ decays allows for unambiguous detection of the fission isomers.

After the daily conclusion of the in-beam measurements, energy spectra of the γ rays emitted by the target are taken overnight. These spectra are examined for background in the regions of interest, including long-lived activation of the target. The 1313.0-keV region is free of background; however, a small background is present at 1279.1 keV. This background is subtracted when calculating the ^{134m}Te yield and only results in an approximately 3% decrease in the total yield.

For the final measurement of the ratio $^{134m}\text{Te}/(^{136m}\text{Xe} + ^{136}\text{I})$, all events occurring in the window from 16 to 162 ns after the beam pulse are used. The yields of the two γ rays lines are extracted by fitting the background and integrating the peak counts. Each target is measured for between 2 and 17 h of beam time and produces between 1500 and 20 000 net counts in the regions of interest.

The ratio of yields is favored over absolute yield determination as it reduces systematic uncertainties, including the beam flux, detector efficiency, effective target mass, attenuation, and self-absorption. The reported ratios are dominated by statistical uncertainties, which can be reduced by using more beam time or a higher beam-target luminosity. The ability to identify the actinide by the measured ratio is not sensitive to the physical attributes of the target. The time signature of the γ decay cannot be altered by any physics mechanism. Gamma rays are highly sensitive to attenuation effects, which is why it is highly desirable for the energy signature of the two γ rays to be substantially close to each other. If the γ rays had largely different energies, the detection efficiency of the two γ rays could be very different and they could be attenuated differently depending on the target geometry and shielding configurations. The data are corrected for the difference in HPGe detector efficiency from 1279.1 to 1313.0 keV. For most γ -ray detectors, including the ones used in the present experiment, the detection efficiency does not noticeably change over this small energy range and this correction is not necessary.

The reported ratios represent the isomer yield at $t = 0$, immediately after the beam pulse, that is, the isomer production yield following fission. Given the difference in half-life of the two isomers, corrections for the counting and decay time are made. The production and decay of the isomers is modeled using cyclic activation analysis with a pulsed beam [27–29] to determine a correction factor of 1.038 for the ratio of yields. The ratios are multiplied by this factor to give the ratio of the $t = 0$ isomer yield. This correction is identical for all targets and energies and does not change the separation between the three actinides but only the overall normalization. For this correction, we assess a $\pm 5\%$ systematic uncertainty caused by the limited timing resolution of the HPGe detectors. There is an additional $\pm 6.5\%$ systematic uncertainty due to the uncertainty on the reported half-life of ^{134m}Te . This gives a total systematic uncertainty of $\pm 8.2\%$.

IV. RESULTS AND DISCUSSION

The ratios of the yield of the fission products $^{134m}\text{Te}/(^{136m}\text{Xe} + ^{136}\text{I})$ for photon-induced fission of ^{235}U , ^{238}U , and ^{239}Pu measured in this work at three photon-beam energies are shown in Fig. 5. The ratio is shown to be highly dependent on the fissioning nucleus. Furthermore, the ratio is relatively constant for incident photons in the

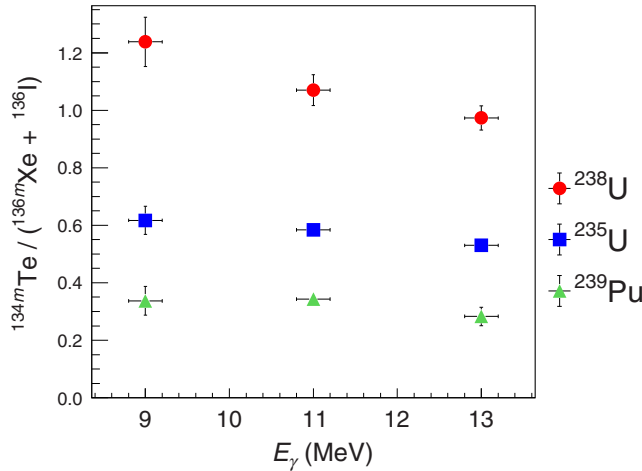


FIG. 5. The plot of the ratios of the fission yields for the $^{134m}\text{Te}/(^{136m}\text{Xe} + ^{136}\text{I})$ measured in this work. This ratio is computed from the ratio of the yields for the 1279.1- and 1313.0-keV γ rays. The vertical error bars represent only the statistical uncertainty. The systematic uncertainty ($\pm 8.2\%$) is identical for all data points, as discussed in the text. The horizontal error bars represent the beam energy spread.

(9–13)-MeV energy range, changing by less than 20% over this energy range.

As the measured ratio does not have a strong energy dependence, the same results could be achieved using a bremsstrahlung beam. Given that the photofission cross section is increasing over this energy range, the product of the bremsstrahlung flux and cross section will be maximized near the bremsstrahlung end-point energy, as shown in Fig. 6 for a hypothetical 8-MeV-endpoint bremsstrahlung beam. Although the resulting excitation energy of the fissioning nucleus is noticeably wider than the $\text{HI}\gamma\text{S}$ beam profile used in the present work, it still shows a peak structure focused around 7.0 ± 1.0 MeV. Nonetheless, a much broader bremsstrahlung beam can potentially produce background from other sources, lowering the signal-to-background ratio. Bremsstrahlung beams will also induce a higher radiological dose than a monoenergetic or Compton-backscattered beam [30].

The present results may be interpolated for different enrichment levels of $^{235,238}\text{U}$ by using the photofission cross sections from Ref. [24], as is shown in Fig. 7. At lower photon energies, the ratio becomes a more sensitive probe of the isotopic composition of the target. This is a desirable feature when combined with the previously discussed aspects of a bremsstrahlung-beam-based experiment.

We now discuss the feasibility of an active interrogation scheme utilizing an 8-MeV-endpoint high-flux bremsstrahlung beam of $10^{10}\gamma/\text{s}$. The use of lower photon energies will, of course, result in a lower fission count rate. By scaling our observed count rates, detector efficiencies,

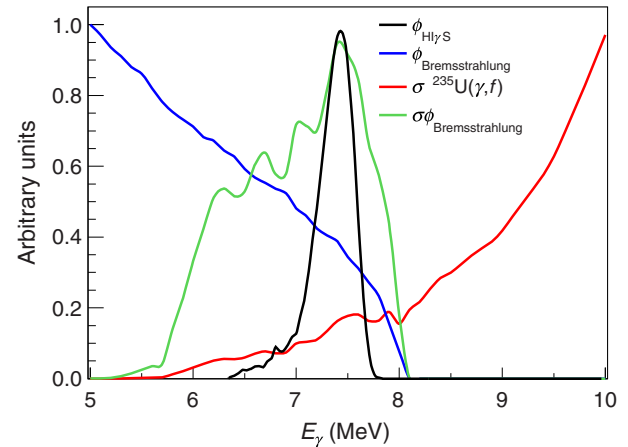


FIG. 6. The relative flux of the $\text{HI}\gamma\text{S}$ beam at 7.5 MeV (black curve) is shown in comparison to a bremsstrahlung beam with an 8-MeV endpoint (blue curve). The bremsstrahlung spectrum is convoluted with the ^{235}U photofission cross section (red curve), to produce the excitation function of the fissioning ^{235}U nucleus (green curve).

detector solid-angle coverage, and beam flux and using the photofission cross section [24], we can make performance estimates for this system. We assume the same pulsing structure of the $\text{HI}\gamma\text{S}$ beam, although a pulsing period of approximately $10\ \mu\text{s}$ would be optimum for measuring the ^{136m}Xe isomer decay and distinguishing it from other contributions, including ^{136}I . We follow the recommended maximum inspection dimensions of Ref. [10] and assume that the detection efficiency scales linearly with the number of detectors utilized, scaling up from the three HPGe detectors used in the present work. For a small object (such as a carry-on or suitcase), where the target is positioned 0.3 m from an array of ten HPGe detectors, this configuration could measure the $^{134m}\text{Te}/^{136m}\text{Xe}$ ratio to 10% accuracy in

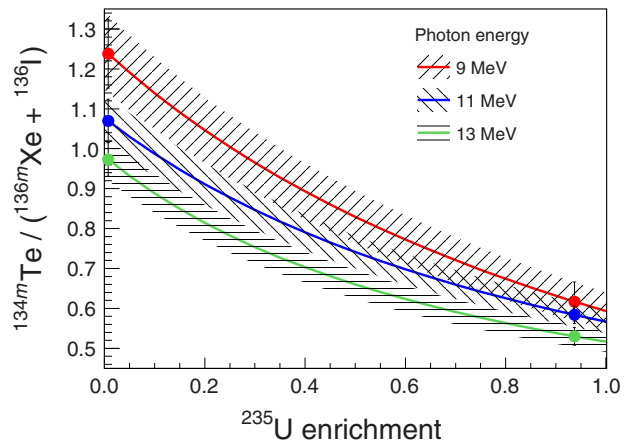


FIG. 7. The reported ratio interpolated as a function of enrichment for a pure $^{235,238}\text{U}$ system. The two measured enrichment levels are shown by the solid circle points.

31 s per gram of material, or 3% accuracy in 344 s per gram of material. For interrogation of an intermodal cargo container, where the target material is located 2.6 m from an array of 30 HPGe detectors, the proposed system could measure the present ratio to 10% accuracy in 1 s per kilogram of material, or 3% accuracy in 9 s per kilogram of material. When considering kilogram-scale quantities, it should be noted that bulk uranium has a 0.87-cm attenuation length at 1.3 MeV [26], so the present technique will only probe the surface to a depth of approximately 0.5 cm. For a spherical 25-kg target material (as recommended in Ref. [10]), this results in a measurement of only the outer 2.5 kg, reducing the sensitivity by a factor of 10. Similarly, for a spherical 5-kg target mass, this technique would only probe the outer approximately 0.83 kg, resulting in a reduction in sensitivity by a factor of 6. In these scenarios, the bremsstrahlung source and γ -ray detector are required to be oriented facing the same target surface. Probing deeper into a sample material, if needed, would likely require neutron-based techniques. These count rates are calculated and scaled from our experiment and the available nuclear data. Additional considerations, such as the detector background levels, the detector dead time incurred by the use of a high-flux beam, and the attenuation of the signal 1.3-MeV γ rays, are not included in the present calculations. A detailed Monte Carlo study is necessary to further assess the feasibility of the present technique.

Practical application of the present work necessitates a discussion of backgrounds. As has already been stated, these isomers have a unique time and energy signature, which permits them to be distinguished from most γ -ray backgrounds. The present time window occurs after prompt radiation but before β decay. In this specific time window, induced nuclear isomeric decays are the primary source of background. The vast majority of nuclear isomers exist either due to a low excitation energy or a large spin difference from the ground state. When using a photon-beam probe, it is highly unlikely that the $J = 1$ photon will populate these high-spin states. The (γ, n) and (γ, p) reactions are more likely to produce isomeric states, which necessitates staying below the particle-separation thresholds during practical applications. Below these thresholds, fission becomes the only nuclear process capable of producing high-spin isomers. Depending on the beam repetition rate and exposure time, a buildup of longer-lived fission products will eventually begin to substantially increase the background γ spectra of the actinide target, as can be seen by the background levels in Fig. 4 for the present data. In this sense, shorter irradiations performed with higher flux are preferable.

V. CONCLUSIONS

Using pulsed and monoenergetic beams from the HI γ S facility, fissions are induced during the beam-on periods,

while decays from the ^{134m}Te and ^{136m}Xe fission-product isomers are observed during the beam-off periods. Our studies show that natural background radiation, activation products, and β -decaying fission products have long decay half-lives compared to the isomeric decays. The fast decay time scale for these isomers allows a clean signal to be collected quickly. These findings indicate that detection of isomers produced in fission is a promising technique for active interrogation of special nuclear materials. The yields are comparable to those of β -delayed neutrons but have multiple advantages: radiation occurs over a shorter time period, the radiation has a monoenergetic energy spectrum, the decays give information about the identity of the fissioning material, and the time scale for applications in beam-based material interrogation is compatible with that used in prompt-fission neutron detection. Even for γ -ray detectors with poor energy resolution, such as NaI or CeBr₃, where the γ -ray transitions from ^{134m}Te and ^{136m}Xe could overlap, their yield can still be extracted from the time decay data. The ratio $^{134m}\text{Te}/^{136m}\text{Xe}$ is an attractive diagnostic in that the identity of the fissioning species may be ascertained without any knowledge of the beam flux, the number of fissions induced in the target, the detection efficiency, or the attenuation factors. For practical applications, multiple forms of prompt and delayed radiation could be detected, increasing the sensitivity and accuracy for identifying special nuclear materials.

ACKNOWLEDGMENTS

This work was supported in part by the Grants No. DE-NA0002793 and No. DE-NA0003887 and the U.S. Department of Energy, Office of Nuclear Physics, under Grant No. DE-FG02-97ER41033. The work was also performed under the auspices of the U.S. Department of Energy by the Lawrence Livermore National Laboratory under Contract No. DE-AC52-07NA27344 and by Los Alamos National Security, LLC under Contract No. DE-AC52-06NA25396.

-
- [1] R. Vandenbosch and J. R. Huizenga, *Nuclear Fission* (Academic Press, New York, 1973), p. xii, 422 p.
 - [2] J. B. Wilhelmy, E. Cheifetz, R. C. Jared, S. G. Thompson, H. R. Bowman, and J. O. Rasmussen, Angular momentum of primary products formed in the spontaneous fission of ^{252}Cf , *Phys. Rev. C* **5**, 2041 (1972).
 - [3] H. Naik, S. P. Dange, and R. J. Singh, Angular momentum of fission fragments in low energy fission of actinides, *Phys. Rev. C* **71**, 014304 (2005).
 - [4] I. Stetcu, P. Talou, T. Kawano, and M. Jandel, Properties of prompt-fission γ rays, *Phys. Rev. C* **90**, 024617 (2014).
 - [5] W. John, F. W. Guy, and J. J. Wesolowski, Four-parameter measurements of isomeric transitions in ^{252}Cf fission fragments, *Phys. Rev. C* **2**, 1451 (1970).
 - [6] K. Siegl, K. Kolos, N. D. Scielzo, A. Aprahamian, G. Savard, M. T. Burkley, M. P. Carpenter, P. Chowdhury, J.

- A. Clark, P. Copp, G. J. Lane, C. J. Lister, S. T. Marley, E. A. McCutchan, A. J. Mitchell, J. Rohrer, M. L. Smith, and S. Zhu, β -decay half-lives of $^{134,134m}\text{Sb}$ and their isomeric yield ratio produced by the spontaneous fission of ^{252}Cf , *Phys. Rev. C* **98**, 054307 (2018).
- [7] A. A. Sonzogni, Nuclear data sheets for $A = 134$, *Nucl. Data Sheets* **103**, 1 (2004).
- [8] E. A. McCutchan, Nuclear data sheets for $A = 136$, *Nucl. Data Sheets* **152**, 331 (2018).
- [9] P. Talou, T. Kawano, I. Stetcu, J. P. Lestone, E. McKigney, and M. B. Chadwick, Late-time emission of prompt fission γ rays, *Phys. Rev. C* **94**, 064613 (2016).
- [10] American national standard minimum performance criteria for active interrogation systems used for homeland security, ANSI N42.41-2007, p. 1 (2008).
- [11] R. C. Runkle, D. L. Chichester, and S. J. Thompson, Rattling nucleons: New developments in active interrogation of special nuclear material, *Nucl. Instrum. Methods A* **663**, 75 (2012).
- [12] B. J. Quiter, B. A. Ludewigt, V. V. Mozin, C. Wilson, and S. Korbly, Transmission nuclear resonance fluorescence measurements of ^{238}U in thick targets, *Nucl. Instrum. Methods B* **269**, 1130 (2011).
- [13] M. S. Johnson, C. A. Hagmann, J. M. Hall, D. P. McNabb, J. H. Kelley, C. Huibregtse, E. Kwan, G. Rusev, and A. P. Tonchev, Searching for illicit materials using nuclear resonance fluorescence stimulated by narrow-band photon sources, *Nucl. Instrum. Methods B* **285**, 72 (2012).
- [14] E. Kwan, G. Rusev, A. S. Adekola, F. Dönau, S. L. Hammond, C. R. Howell, H. J. Karwowski, J. H. Kelley, R. S. Pedroni, R. Raut, A. P. Tonchev, and W. Tornow, Discrete deexcitations in ^{235}U below 3 MeV from nuclear resonance fluorescence, *Phys. Rev. C* **83**, 041601 (2011).
- [15] S. L. Hammond, A. S. Adekola, C. T. Angell, H. J. Karwowski, E. Kwan, G. Rusev, A. P. Tonchev, W. Tornow, C. R. Howell, and J. H. Kelley, Dipole response of ^{238}U to polarized photons below the neutron separation energy, *Phys. Rev. C* **85**, 044302 (2012).
- [16] E. B. Norman, S. G. Prusin, R. Larimer, H. Shugart, E. Browne, A. R. Smith, R. J. McDonald, H. Nitsche, P. Gupta, M. I. Frank, and T. B. Gosnell, Signatures of fissile materials: High-energy γ rays following fission, *Nucl. Instrum. Methods A* **521**, 608 (2004).
- [17] F. Carrel, M. Agelou, M. Gmar, F. Laine, J. Lordin, J. L. Ma, C. Passard, and B. Poumarede, Identification and differentiation of actinides inside nuclear waste packages by measurement of delayed gammas, *IEEE Trans. Nucl. Sci.* **57**, 2862 (2010).
- [18] A. Iyengar, E. B. Norman, C. Howard, C. Angell, A. Kaplan, J. J. Ressler, P. Chodash, E. Swanberg, A. Czeszumska, B. Wang, R. Yee, and H. A. Shugart, Distinguishing fissions of ^{232}Th , ^{237}Np and ^{238}U with beta-delayed gamma rays, *Nucl. Instrum. Methods B* **304**, 11 (2013).
- [19] A. Sari, F. Carrel, F. Lainé, and A. Lyoussi, Neutron interrogation of actinides with a 17 MeV electron accelerator and first results from photon and neutron interrogation non-simultaneous measurements combination, *Nucl. Instrum. Methods B* **312**, 30 (2013).
- [20] J. Nattress, K. Ogren, A. Foster, A. Meddeb, Z. Ounaies, and I. Jovanovic, Discriminating Uranium Isotopes Using the Time-Emission Profiles of Long-Lived Delayed Neutrons, *Phys. Rev. Appl.* **10**, 024049 (2018).
- [21] T. Gozani, J. Bendahan, M. J. King, C. Brown, M. Elsalim, and E. Elias, Differential time of flight technique for the detection of special nuclear materials, *IEEE Trans. Nucl. Sci.* **60**, 1118 (2013).
- [22] J. M. Mueller, M. W. Ahmed, and H. R. Weller, A novel method to assay special nuclear materials by measuring prompt neutrons from polarized photofission, *Nucl. Instrum. Methods A* **754**, 57 (2014).
- [23] J. M. Mueller, M. W. Ahmed, A. Kafkarkou, D. P. Kendellen, M. H. Sikora, M. C. Spraker, H. R. Weller, and W. R. Zimmerman, Tests of a novel method to assay snm using polarized photofission and its sensitivity in the presence of shielding, *Nucl. Instrum. Methods A* **776**, 107 (2015).
- [24] D. A. Brown, M. B. Chadwick, R. Capote, A. C. Kahler, A. Trkov, M. W. Herman, A. A. Sonzogni, Y. Danon, A. D. Carlson, M. Dunn, *et al.*, ENDF/B-VIII.0: The 8th major release of the nuclear reaction data library with CIELO-project cross sections, new standards and thermal scattering data, *Nucl. Data Sheets* **148**, 1 (2018), special Issue on Nuclear Reaction Data.
- [25] H. R. Weller, M. W. Ahmed, H. Gao, W. Tornow, Y. K. Wu, M. Gai, and R. Miskimen, Research opportunities at the upgraded HI γ S facility, *Progr. Part. Nucl. Phys.* **62**, 257 (2009).
- [26] M. J. Berger, J. H. Hubbell, S. M. Seltzer, J. Chang, J. S. Coursey, R. Sukumar, D. S. Zucker, K. Olsen, XCOM, Photon Cross Section Database (version 1.5). [Online] Available: <http://physics.nist.gov/xcom> [2020, July 30]. National Institute of Standards and Technology, Gaithersburg, MD. (2010).
- [27] N. S. Chen and J. H. Fremlin, Activation analysis by pulsed cyclotron beams, *Nucl. Instrum. Meth.* **85**, 61 (1970).
- [28] W. W. Givens, W. R. Mills, and R. L. Caldwell, Cyclic activation analysis, *Nucl. Instrum. Methods* **80**, 95 (1970).
- [29] N. M. Spyrou, Cyclic activation analysis—A review, *J. Radioanal. Chem.* **61**, 211 (1981).
- [30] J. Pruet, D. P. McNabb, C. A. Hagmann, F. V. Hartemann, and C. P. J. Barty, Detecting clandestine material with nuclear resonance fluorescence, *J. App. Phys.* **99**, 123102 (2006).